

**Magnetism and chemical ordering in binary transition metal clusters**

Georg Rollmann, Sanjubala Sahoo, Alfred Hucht, and Peter Entel

*Physics Department, University of Duisburg-Essen, Lotharstrasse 1, 47048 Duisburg, Germany*

(Received 24 September 2007; published 3 October 2008)

Binary  $XY$  clusters, with  $X, Y \in \{\text{Mn, Fe, Co, Ni}\}$ , are investigated within first-principles simulations in the framework of density-functional theory. In the case of Co-Mn, the increase in magnetic moment with Mn concentration, which is in contrast to the bulk behavior and was also observed experimentally, is explained on the basis of the electronic structure of the clusters. For Co-Fe, Ni-Mn, Ni-Fe, and Ni-Co, due to the ferromagnetic couplings between the local moments, the same dependence is found, i.e., moments increasing with the concentration of the element with the lower value of atomic number. For Fe-Mn (as well as Co-Mn and Ni-Mn clusters containing many Mn atoms), the situation appears to be more complex with antiferromagnetic tendencies resulting in a nonmonotonic change of the cluster moment with Mn concentration.

DOI: [10.1103/PhysRevB.78.134404](https://doi.org/10.1103/PhysRevB.78.134404)

PACS number(s): 36.40.Cg, 61.46.Bc, 61.46.Df

**I. INTRODUCTION**

Magnetic transition metal (TM) nanoclusters are currently receiving considerable attention from a fundamental, as well as a technological, point of view, being discussed as promising candidates for future applications such as, e.g., ultrahigh density magnetic storage devices.<sup>1</sup> Due to their reduced dimensionality, many of their properties significantly differ from those of the corresponding bulk materials. This gives rise to numerous interesting phenomena, such as unusually high magnetic moments<sup>2</sup> or unique geometric structures.<sup>3,4</sup>

In going from monoatomic to binary systems, composition and atomic arrangement in the clusters, e.g., core-shell as opposed to other ordered structures or random alloys,<sup>5</sup> provide additional degrees of freedom, which open up the possibility to design new materials with desired properties. Today it has become feasible to conduct experiments in which some of these properties are measured on an atomic level.<sup>6–8</sup> In the case of Co-Mn, it could be shown recently that the clusters possess different magnetic properties than bulk Co-Mn: While in the latter, on the Co-rich side, the moment decreases with increasing Mn concentration  $x_{\text{Mn}}$ , an increase is found for the clusters.<sup>8</sup> In contrast to that, the behavior of clusters matches that of the volume material in the Co-V system. The unexpected finding for the Co-Mn clusters was interpreted on the basis of a Friedel-type picture<sup>9</sup> for their electronic densities of states. Without having access to these in experiment, however, no definite explanation could be given. Furthermore, the experiments could only be performed for Co-rich clusters, i.e., for  $x_{\text{Mn}} < 0.4$ . To our knowledge, comparable studies have not been reported of yet for other combinations of TM elements.

Due to the substantial numerical effort arising from the fact that the presence of more than one species in the clusters greatly enhances the complexity of the problem, computational studies for polyatomic clusters were, in the past, either performed using model potentials,<sup>10,11</sup> restricted to selected compositions,<sup>11–13</sup> or smaller systems with only a handful of atoms.<sup>14</sup> In this work, we present results from a systematic *ab initio* investigation over the whole composition range for 13-atom binary TM clusters composed of the elements Mn, Fe, Co, and Ni, as well as 55-atom Co-Mn clusters. The

findings enable us to unravel the mechanism responsible for the magnetism in small Co-Mn clusters and at the same time obtain information about magnetic properties and ordering in the other TM systems for which only limited experimental or theoretical information is available.

**II. COMPUTATIONAL DETAILS**

The calculations were performed within density-functional theory in the generalized gradient approximation (GGA) parametrized by Perdew, Burke, and Ernzerhof<sup>15</sup> in combination with the projector-augmented wave method<sup>16</sup> and a plane-wave basis set. This approach has proven to be able to successfully describe the atomic systems treated here: The accuracy of the projector-augmented wave method is comparable to an all-electron calculation, and a plane-wave basis set can be considered superior to localized basis functions as it allows for a smooth, systematic convergence of calculated quantities with basis-set size. While it is definitely necessary to go beyond the local-density approximation and take into account gradient corrections, the specific choice of GGA functional, however, leaves calculated energetic and magnetic properties of TM systems essentially unaffected.<sup>17–19</sup>

It turned out that, for the present investigation, relativistic effects could be neglected, as well as noncollinear magnetic states, which only play a role in the high- $x_{\text{Mn}}$  regime. We have also checked that explicit consideration of electronic correlation effects (GGA+ $U$ ) does not change the ground states, except for a slight increase in total magnetic moments. These three aspects are discussed in more detail in Sec. III. With respect to the interaction of the clusters with their periodic images, cubic supercells of 12 Å and 18 Å length proved to be sufficiently large. All simulations were carried out with the Vienna *ab-initio* simulation package (VASP).<sup>20,21</sup>

In order to systematically explore the effect of chemical ordering and composition on the cluster properties, we focus on closed-shell icosahedra with 13 and 55 atoms, which are found to be particularly stable for the TM clusters considered here.<sup>6,22</sup> However, there are still 164 possibilities to distribute two kinds of atoms over the sites of a 13-atom icosahedron. In addition, many different spin multiplicities had to be

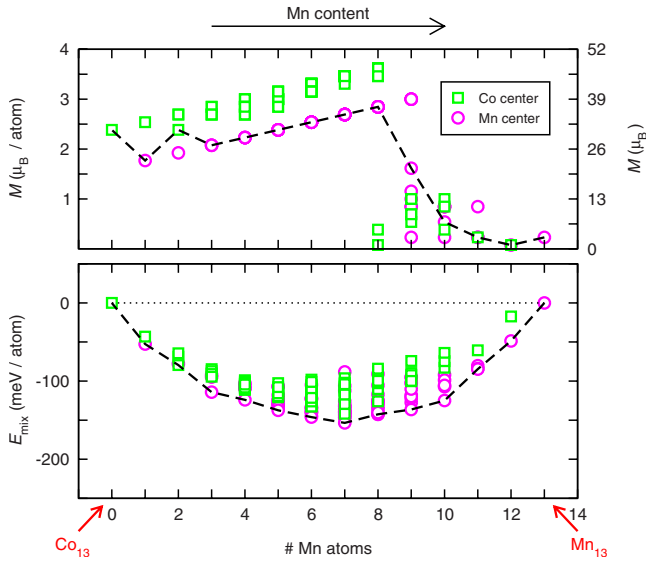


FIG. 1. (Color online) Magnetic moments (top panel) and relative energies (bottom panel) for the 164 isomers of icosahedral 13-atom Co-Mn clusters. Isomers with a Mn atom at the center are represented by circles (magenta), clusters with a Co atom at the center with squares (green). The black lines mark the lowest-energy isomers found for each composition.

taken into account for each of these homotopes. For the resulting clusters, geometric optimizations without imposing any symmetry constraints were performed with the conjugate-gradient method until the forces were below  $1 \text{ meV}/\text{\AA}$ . For 55-atom icosahedral clusters, we have studied a limited composition range due to the huge number of possible distributions of the atoms that leads to more than  $10^{14}$  different homotopes.

### III. RESULTS AND DISCUSSION

We begin our discussion with the Co-Mn system. Upon relaxation, all isomers retain their overall icosahedral shape, with slight distortions originating from the difference in atomic volume of Co and Mn atoms, as well as Jahn-Teller instabilities of some highly symmetric isomers. In Fig. 1, magnetic moments and mixing energies,

$$E_{\text{mix}}(n) = E^{A_{N-n}B_n} - \left( \frac{N-n}{N} E^{A_N} + \frac{n}{N} E^{B_N} \right), \quad (1)$$

are depicted. The negative values of  $E_{\text{mix}}$  over the whole composition range indicate the favorable solubility of the components, the most stable isomers being found for about an equal amount of Co and Mn atoms. In the lowest-energy isomers, with the exception of  $\text{Co}_{11}\text{Mn}_2$ , where the two Mn atoms prefer opposite positions on the icosahedral shell, the central position of the icosahedron is occupied by a Mn atom. The remaining Mn atoms tend to achieve maximum distance from each other on the cluster surface. Substituting a Co by a Mn atom at the center results in a drop of  $8\mu_B$  in magnetic moment, which directly corresponds to the case of bulk Co-Mn with small  $x_{\text{Mn}}$ . However, irrespective of the type of central atom, substitution of a Co atom by a Mn atom

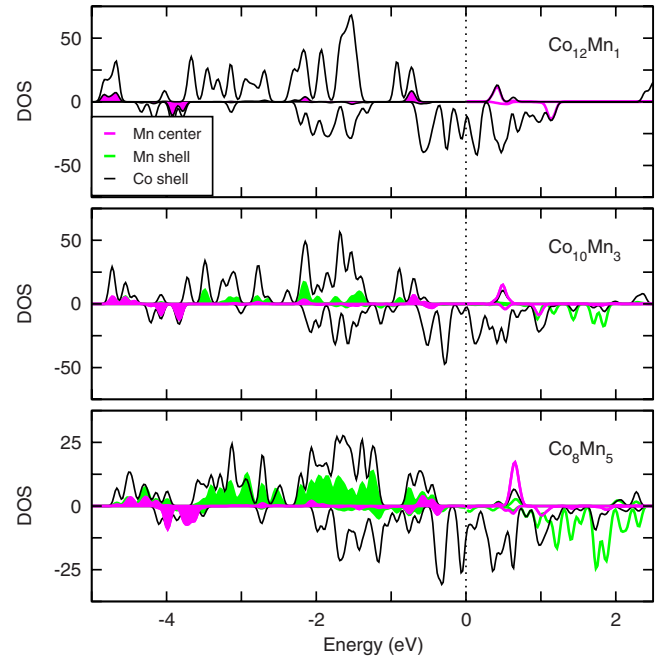


FIG. 2. (Color online) Change of the site-projected electronic density of states of 13-atom Co-Mn clusters with Mn concentration. Occupied Mn states are shaded. The  $\delta$  peaks of the energy levels have been smeared using a value of  $50 \text{ meV}$ . The scale of the bottom panel has been changed in favor of better readability of the figure.

at the surface increases the spin multiplicity by two, resulting in an increase in the total magnetic moment by  $2\mu_B$ , up to a number of eight Mn atoms in the cluster. This finding is in perfect agreement with the behavior of Co-Mn clusters of various sizes observed experimentally,<sup>8</sup> and is also supported by very recent results of a computational study<sup>23</sup> that has appeared during the publication process of the present paper.

At  $\text{Co}_5\text{Mn}_8$ , a crossover from ferromagnetic (FM) coupling of the surface atoms to antiferromagnetic (AF)-like ordering takes place. This is due to the fact that the spin structures of the pure clusters are completely different: While the local moments are aligned in parallel in  $\text{Co}_{13}$ , the moments of six surface atoms are flipped in  $\text{Mn}_{13}$ , leading to a very small total moment of only  $3\mu_B$ . When a few Mn atoms are replaced by Co, the AF-like order is conserved. This is in good agreement with a previous study on pure Mn clusters,<sup>24</sup> where the switch from FM to AF was found to occur for  $\text{Mn}_5$ —an entity which is practically not present in 13-atom Co-Mn clusters containing less than eight Mn atoms. Due to the vast number of possible spin configurations for the AF-like isomers, a comprehensive account of the ground-state properties in the high- $x_{\text{Mn}}$  regime is beyond the scope of this work.

The absolute values of the local moments of the surface Mn atoms in  $\text{Mn}_{13}$  as well as in the mixed clusters are, with  $\sim 4.1\mu_B$ , more than  $1.5\mu_B$  larger than those of the Co atoms in  $\text{Co}_{13}$ , indicating that they largely retain their atomic character. This is illustrated in Fig. 2, where the change of the electronic structure of the lowest-energy isomers with the number of Mn atoms is displayed. In all these isomers, the moment of the central Mn atom is quenched, which results,

together with a reduction in the moments of the surrounding Co atoms, in the moment drop when the central Co atom is replaced by Mn—exactly like in the bulk.<sup>7</sup> However, the Mn shell atoms couple FM to the Co atoms. Their large magnetic moments originate from the  $3d$  majority spin states located between  $-3$  and  $-1$  eV below the Fermi energy. Due to the large exchange splitting, the corresponding minority spin states are unoccupied and lie about 4 eV higher. A discussion related to many-body effects is omitted here, since with increasing  $x_{\text{Mn}}$ , spectral weight is distributed over the whole energy range.

A topic that has been discussed extensively especially in connection with Co and Mn atoms is that of noncollinear magnetic structures. In the framework of the computational scheme described in Ref. 25, we have relaxed the electronic states, as well as the atomic positions of several mixed clusters starting from different, noncollinear initial spin structures. However, it turned out that noncollinearity does not play a role here, as collinear magnetic structures were again obtained for all the isomers we considered. This is in agreement with a finding for pure Fe clusters where the stability of noncollinear states is lost when the atoms are allowed to relax and cluster symmetry is broken.<sup>26</sup> We have also investigated the influence of relativistic effects by performing additional calculations for the whole composition range where spin-orbit interaction is treated as a perturbation term in the scalar-relativistic Hamiltonian. It turns out that, in contrast to the spin moments, the orbital moments decrease with increasing Mn-atom concentration. However, irrespective of the cluster composition, they are more than one order of magnitude smaller and do not change the trends discussed above.

In order to find out whether the behavior observed for the 13-atom clusters is also maintained in larger systems, we have considered 55-atom Co-Mn clusters made up from a central atom and two icosahedral shells. Due to the huge number of possible distributions of the atoms, it is not possible to perform a similar comprehensive investigation as in the 13-atom case. We opted to study the low- $x_{\text{Mn}}$  range with up to twelve Mn atoms in the clusters, for which experimental data are available.<sup>8</sup> While we were able to consider all possible homotopes for  $\text{Co}_{54}\text{Mn}_1$  (4) and  $\text{Co}_{53}\text{Mn}_2$  (31), we have investigated ten randomly chosen, as well as up to five homotopes constructed by hand for  $\text{Co}_{52}\text{Mn}_3$  to  $\text{Co}_{43}\text{Mn}_{12}$ .

Magnetic moments and relative energies obtained after full structural optimizations of these 177 different isomers are shown in Fig. 3. In the lowest-energy structures among these, most of the Mn atoms occupy surface positions far away from each other and, as a result, possess many Co atoms as nearest neighbors. For some compositions, this is connected to the occupation of the central position with a Mn atom, although the corresponding energy gain is relatively small. In contrast to that, occupation of the inner shell with many Mn atoms results in very unfavorable structures.

The resulting magnetic properties of the 55-atom system are very similar to the 13-atom case. Except some single isomers that are energetically not relevant, the moments of all individual clusters lie in a  $10\mu_B$ -wide stripe with a slope of  $2\mu_B$ , which is bounded from above by isomers with many (more than 50%) Mn atoms at the surface. For clusters with

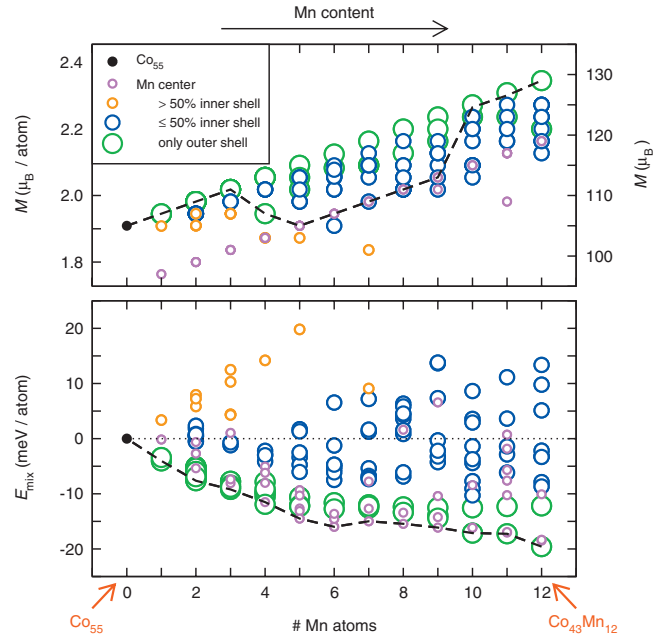


FIG. 3. (Color) Magnetic moments (top panel) and relative energies (bottom panel) for various isomers of icosahedral 55-atom Co-Mn clusters. Different kinds of isomers are distinguished by color; the lowest-energy isomers are marked by a dashed line.

only Co atoms on the inner shell, replacing a Co atom at the center by Mn again results in a drop of  $8\mu_B$ , which again corresponds to the bulk behavior. Although this actually happens in some of the lowest-energy isomers, the overall increase in moment by  $2\mu_B$  per added Mn atom is clearly recognized and is in excellent agreement with the experimental findings. Within this picture, even the slight drop in moment for some cluster sizes at very small  $x_{\text{Mn}}$  observed but not discussed in Ref. 8 can be explained by the first Mn atoms occupying internal positions in the cluster, while the following Mn atoms are then going to the surface.

The electronic density of states for a characteristic 55-atom Co-Mn cluster—the lowest-energy isomer found for  $\text{Co}_{49}\text{Mn}_6$ —is displayed in Fig. 4 (states have been smeared); like in the case of the 13-atom system, the moment of the central Mn atom is quenched due to the strong hybridization with states of the surrounding Co atoms. In contrast to that,

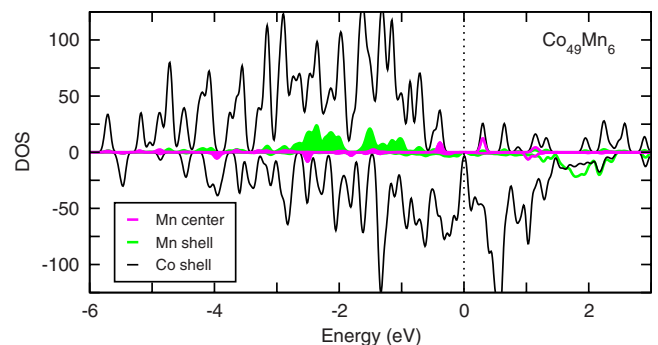


FIG. 4. (Color online) Electronic density of states of a  $\text{Co}_{49}\text{Mn}_6$  cluster, projected onto states of the central Mn atom (magenta), outer shell Mn atoms (green), and Co atoms (black).

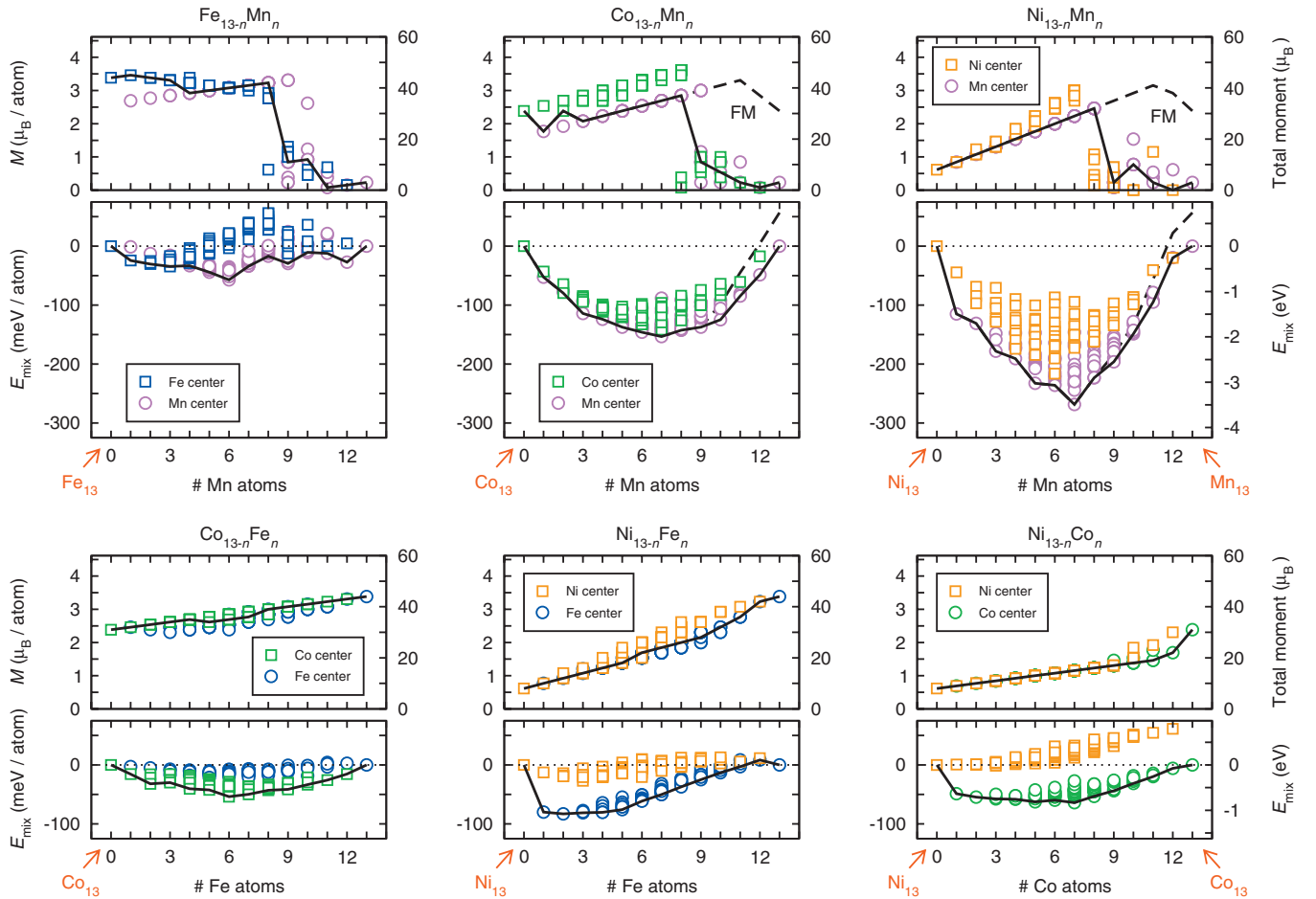


FIG. 5. (Color) Magnetic moments (top panels) and mixing energies (bottom panels) of 13-atom binary TM clusters as a function of composition. For each system, results are divided into two groups according to the element occupying the central position of the icosahedron. Black dashed lines mark the properties of the lowest-energy isomers found for each composition.

the Mn atoms located at the cluster surface possess local magnetic moments of  $\sim 3.9\mu_B$ . They couple FM to the Co atoms, with the Mn  $d$  states lying 4 eV below the corresponding unoccupied minority states.

When we replace Co by Ni, we find the same magnetic behavior as in the Co-Mn system, except that the slope of the moment vs  $x_{\text{Mn}}$  curve now amounts to three, which corresponds to the difference in atomic numbers of Mn and Ni. Preferential occupation of surface sites by the Mn atoms, as well as a crossover to AF-like ordering, is also found for this system. This is shown in Fig. 5, where results from structural optimizations of binary clusters made up from Mn, Fe, Co, and Ni are summarized. In the case of Fe-Mn, no comparable trend is observed, which can be traced back to AF tendencies in this system, making it the most complicated to study. A detailed discussion of the ground-state properties of the individual isomers, however, does not lie in the scope of this work. We only note that the Fe-Mn system is the one with the smallest mixing energy of all. For the combinations of the FM 3d TM elements Fe, Co, and Ni, again an increase in the moment with the concentration of the element with the smaller atomic number  $Z$  is found. In all three cases, one of the elements clearly prefers the central position, however, not always the one with the lower value of  $Z$ .

For comparison with the measurements of Ref. 8, we have also performed calculations for the  $\text{Co}_{13-n}\text{V}_n$  system. Due to the complicated ferrimagnetic spin structures that determine the energy landscapes of these clusters, we were not able to find the configurations with the lowest energy for each cluster (which would require up to several hundreds of calculations for each single isomer). However, even without taking into account subtle details of the spin structures and starting from randomly oriented local moments under the constraint of different fixed spin multiplicities, the experimentally observed picture, namely, the decrease in cluster moment with increasing V concentration, emerges from the calculations in a natural way and is easily explained by the AF coupling of V atoms with the surrounding Co atoms also for low V concentration. This is the behavior expected from the bulk and is in contrast to the Co-Mn case.

We would also like to add some remarks concerning the effects of electronic correlation beyond the GGA that can, e.g., be incorporated in the calculations via the GGA+ $U$  approach.<sup>27</sup> We have shown recently<sup>28</sup> that the explicit consideration of the on-site Coulomb interaction between localized  $d$  electrons is important for very small TM (especially Fe) systems, in which the coordination of the atoms is low (like in  $\text{Fe}_2$ ). While, in that case, calculated ground-state

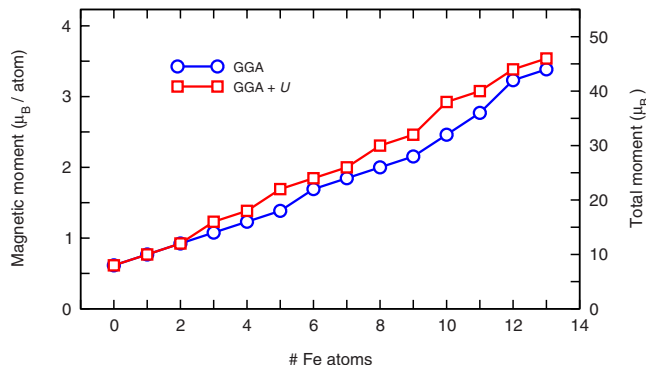


FIG. 6. (Color online) Magnetic moments of 13-atom Ni-Fe clusters, calculated within GGA (blue circles), as well as GGA+ $U$  with  $U_{\text{Ni}}=3$  eV and  $U_{\text{Fe}}=2$  eV (red squares).

properties can be affected significantly, the GGA+ $U$  treatment is far less important in larger systems, metallic systems, where the screening of the  $3d$  electrons is more pronounced and the density of states already shows bulk-like features. This is illustrated in Fig. 6, where the change of magnetic moments with composition is compared for GGA and GGA+ $U$  (with  $U_{\text{Ni}}=3$  eV and  $U_{\text{Fe}}=2$  eV) for the lowest-energy isomers of 13-atom icosahedral Ni-Fe clusters. Al-

though for most compositions the magnetic moment of the ground state is 2, 4, or  $6\mu_B$  higher in the GGA+ $U$  case, which can be traced back to subtle changes in the electronic structures of the clusters, the overall behavior is clearly unaffected.

#### IV. CONCLUSION

To summarize, we have shown that the unexpected finding of increasing magnetic moments in binary Co-Mn clusters can be explained by the large surface-to-volume ratio of the clusters, in combination with the fact that the Mn atoms prefer to occupy surface positions, resulting in local moments which are aligned FM with respect to the Co moments. The same behavior is obtained for Co-Fe, Ni-Mn, Ni-Fe, and Ni-Co clusters, while in the case of Fe-Mn, AF tendencies lead to a nonmonotonic change of magnetic moment with  $x_{\text{Mn}}$ .

#### ACKNOWLEDGMENTS

This work was supported by the DFG through SFB 445. Calculations were performed on the Blue Gene/L system at the NIC in Jülich and the Regional Computer Center of the University of Cologne (RRZK).

- <sup>1</sup>S. Sun, C. B. Murray, D. Weller, L. Folks, and A. Moser, *Science* **287**, 1989 (2000).
- <sup>2</sup>I. M. L. Billas, A. Châtelain, and W. A. de Heer, *Science* **265**, 1682 (1994).
- <sup>3</sup>M. Baletto and R. Ferrando, *Rev. Mod. Phys.* **77**, 371 (2005).
- <sup>4</sup>G. Rollmann, M. E. Gruner, A. Hucht, R. Meyer, P. Entel, M. L. Tiago, and J. R. Chelikowsky, *Phys. Rev. Lett.* **99**, 083402 (2007).
- <sup>5</sup>M. E. Gruner, G. Rollmann, P. Entel, and M. Farle, *Phys. Rev. Lett.* **100**, 087203 (2008).
- <sup>6</sup>G. M. Koretsky, K. P. Kerns, G. C. Nieman, M. B. Knickelbein, and S. J. Riley, *J. Phys. Chem. A* **103**, 1997 (1999).
- <sup>7</sup>M. B. Knickelbein, *Phys. Rev. B* **75**, 014401 (2007).
- <sup>8</sup>S. Yin, R. Moro, X. Xu, and W. A. de Heer, *Phys. Rev. Lett.* **98**, 113401 (2007).
- <sup>9</sup>J. Friedel, *Nuovo Cimento, Suppl.* **7**, 287 (1958).
- <sup>10</sup>E. F. Rexer, J. Jellinek, E. B. Krissinel, E. K. Parks, and S. J. Riley, *J. Chem. Phys.* **117**, 82 (2002).
- <sup>11</sup>A. A. Dzhurakhalov and M. Hou, *Phys. Rev. B* **76**, 045429 (2007).
- <sup>12</sup>B. K. Rao, S. Ramos de Debiaggi, and P. Jena, *Phys. Rev. B* **64**, 024418 (2001).
- <sup>13</sup>G. Rollmann, S. Sahoo, and P. Entel, *Phys. Status Solidi A* **201**, 3263 (2004).
- <sup>14</sup>M. Harb, F. Rabilloud, and D. Simon, *J. Phys. Chem. A* **111**, 7726 (2007).
- <sup>15</sup>J. P. Perdew, K. Burke, and M. Ernzerhof, *Phys. Rev. Lett.* **77**, 3865 (1996).
- <sup>16</sup>P. E. Blöchl, *Phys. Rev. B* **50**, 17953 (1994).
- <sup>17</sup>C. J. Barden, J. C. Rienstra-Kiracofe, and H. F. Schaefer III, *J. Chem. Phys.* **113**, 690 (2000).
- <sup>18</sup>S. Yanagisawa, T. Tsuneda, and K. Hirao, *J. Chem. Phys.* **112**, 545 (2000).
- <sup>19</sup>G. L. Gutsev and C. W. Bauschlicher, Jr., *J. Phys. Chem. A* **107**, 7013 (2003).
- <sup>20</sup>G. Kresse and J. Furthmüller, *Phys. Rev. B* **54**, 11169 (1996).
- <sup>21</sup>G. Kresse and D. Joubert, *Phys. Rev. B* **59**, 1758 (1999).
- <sup>22</sup>M. Pellarin, B. Baguenard, J. L. Vialle, J. Lerme, M. Broyer, J. Miller, and A. Perez, *Chem. Phys. Lett.* **217**, 349 (1994).
- <sup>23</sup>S. Ganguly, M. Kabir, S. Datta, B. Sanyal, and A. Mookerjee, *Phys. Rev. B* **78**, 014402 (2008).
- <sup>24</sup>G. L. Gutsev, M. D. Mochena, and C. W. Bauschlicher, *J. Phys. Chem. A* **110**, 9758 (2006).
- <sup>25</sup>D. Hobbs, G. Kresse, and J. Hafner, *Phys. Rev. B* **62**, 11556 (2000).
- <sup>26</sup>G. Rollmann, P. Entel, and S. Sahoo, *Comput. Mater. Sci.* **35**, 275 (2006).
- <sup>27</sup>V. I. Anisimov, J. Zaanen, and O. K. Andersen, *Phys. Rev. B* **44**, 943 (1991).
- <sup>28</sup>G. Rollmann, H. C. Herper, and P. Entel, *J. Phys. Chem. A* **110**, 10799 (2006).